BINARY BCH TURBO CODING PERFORMANCE: UNION BOUND AND SIMULATION RESULTS

S. X. Ng, T. H. Liew, L-L. Yang, [1]L. Hanzo

Dept. of ECS, Univ. of Southampton, SO17 1BJ, UK.
Tel: +44-1703-593 125, Fax: +44-1703-594 508
Email: [1]lh@ecs.soton.ac.uk; http://www-mobile.ecs.soton.ac.uk

ABSTRACT

Turbo codes using short binary BCH codes as component codes are investigated. The bit error rate (BER) performance of the turbo codes is evaluated using binary phase shift keying (BPSK) over additive white Gaussian noise (AWGN) channels. The effects of various concatenated component codes, interleaver size, minimum free-distances, weight-distributions as well as puncturing schemes are investigated using both union-bounding and simulations.

1. INTRODUCTION

Turbo codes achieve a performance close to the Shannon limit[1]. Turbo coding [1, 2, 3, 4, 5] is also referred to as parallel-concatenated coding, since it consists of two parallel constituent systematic encoders linked by an interleaver. The block-turbo encoded sequence consists of the information sequence, the parity bits of the first encoder and the parity bits of the second encoder. Different component codes and puncturing schemes can be employed in order to obtain turbo codes with desired rates. For coding rates around 1/2 typically Recursive Systematic Convolutional (RSC) codes are used as the component codes. However, turbo codes using block codes as the component codes were found to perform better than RSC codes at near-unity coding rates [6].

For a given channel, the parameters affecting the performance of turbo codes include the component codes, the decoding algorithms, the interleaver size and algorithm, the minimum free-distance and weight-distribution of the codes as well as the puncturing scheme. It has been shown in [7] that the average bit error probability of turbo codes is dominated by a high number of medium-distance weight-distribution terms at low Signal-to-noise Ratios (SNRs). By contrast, at high SNRs the performance is predetermined by the relatively low number of low-distance, low-weight distribution terms, since high-distance codewords are rarely encountered in high-SNR channels. It has also been shown that the interleaver size and structure have an explicit effect on the turbo code's performance. At low SNRs, the interleaver size is much more important than its structure, while, at high SNRs, the performance can be improved by appropriately selecting the interleaver structure.

VTC 2000, Tokyo, Japan, 15-18 May, 2000

The financial support of the following organisations is gratefully acknowledged: European Union; EPSRC, Swindon, UK; CWC, Singapore

The intention of this paper is to characterize the performance of short binary BCH block codes as turbo component codes. Our further intention is to illuminate their weight distribution and to study the effects of different distributions on shaping the associated bit error rate (BER) curves to suit various applications. Hence the BER of the turbo codes investigated was evaluated by simulation. The effects of free-distance, interleaver size, puncturing scheme and component codes on the performance was also studied. Furthermore, the weight-distribution of turbo codes and its effects on the bit error probability was evaluated, indicating that most error events were contributed by the first few weight-distribution terms. Our finidings are applicable to arbitrary constituent codes, interleavers and puncturers, although for the sake of maintaining a low complexity, here we considered short codes and interleavers.

2. TURBO ENCODER

The structure of the binary turbo BCH (TBCH) encoder is shown in Fig. 1. Two systematic BCH encoders are used as component codes with an interleaver placed before the second BCH encoder. The interleaver is used to permute

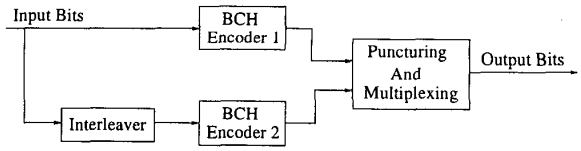

Figure 1: Turbo BCH (TBCH) Encoder Schematic.

the information databits such that the two encoders are operating on the same set of input bits, but - due to the interleaver's randomising effect - on differently ordered input sequences. Therefore the information bits of the 1st BCH encoder are spread into more than one BCH codewords in the 2nd encoder branch. In this contribution block interleaving was invoked. The interleaver size, N was defined as the product of the number of columns, K_1, and the number of rows, K_2 of the interleaver, yielding $N = K_1 \times K_2$, where N is assumed to be divisible by the information-word length, k, so that it could be efficiently filled. Hence, the value of k, which represents the length of information databits of the component codes, determines the choice of the interleaver.

0-7803-5718-3/00/$10.00 ©2000 IEEE.

The turbo codeword consists of the information bits - which are only transmitted once - followed by the parity check bits generated by both encoders. The parity check bits are often punctured according to various puncturing patterns and then multiplexed. Here the aim of puncturing is to obtain a high-rate code, which is implemented by periodically deleting some of the coded bits from a low-rate encoder's output. Hence, by applying puncturing techniques, turbo codes having required code rate can be generated at the cost of coding performance degradation.

3. CODE RATE OF BLOCK TURBO CODES

As an example, a TBCH(7,4,3) code with interleaver size of $N = K_1 \times K_2 = 4 \times 2$, i.e., $K_1 = 4$, $K_2 = 2$ contains two 4-bit words. Viewing the coding scheme of Fig.1 as a single turbo encoder, the length of the information-word to be encoded by the turbo code, K_L, is given by the size of the interleaver, N. However, since each of the two BCH encoders produces $n-k = 3$ parity bits, where n represents the length of the component codes, the total number of parity bits, P_L, of the turbo codeword is given by:

$$P_L = \frac{N}{k} \times 2(n-k), \quad (1)$$

which equals to $P_L = 2 \times 2 \times 3 = 12$ bits in this example. The length of the turbo codeword, L, is given by:

$$\begin{aligned} L &= K_L + P_L \\ &= N + \frac{N}{k} \times 2(n-k), \end{aligned} \quad (2)$$

which equals to $L = 8 + 12 = 20$ bits in our example. Consequently, the code rate for non-punctured turbo codes can be computed by:

$$R = \frac{K_L}{L} = \frac{k}{2n-k}. \quad (3)$$

Eq.(3) implies that the unpunctured turbo code rate is independent of the interleaver size N.

By contrast - in conjunction with puncturing - let us assume that p_w is the number of desirable parity bits after puncturing, which have to be appended to the information-word in order to form a codeword. In other words, p_w indicates the number of parity bits to be retained from the total number of P_L parity bits. Hence, the code rate of punctured block-based turbo codes can be expressed as:

$$R = \frac{N}{N+p_w}, \quad (4)$$

which is explicitly dependent on the puncturing scheme.

4. UNION BOUND OF BIT ERROR PROBABILITY

Let us assume that the turbo encoded bits are transmitted using Binary Phase Shift Keying (BPSK) over the Additive White Gaussian Noise (AWGN) channel. The union bound of the post-decoding BER using trellis-based soft-decision (SD) Viterbi decoding of TBCH codes can be expressed as [8]:

$$p_{bp} = \frac{1}{2N} \sum_{d=d_{min}}^{L} W_d \cdot \mathrm{erfc}\left(\sqrt{\frac{E_b R d}{N_o}}\right), \quad (5)$$

where N is the interleaver size, L is the codeword length of the TBCH code and d_{min} is the minimum Hamming distance between two TBCH codewords. The coefficient W_d is defined as the total number of erroneous information databits in a weight-d path and R is the code rate. Finally, $\mathrm{erfc}(x)$ represents the complementary error function defined as [9]:

$$\mathrm{erfc}(x) = \frac{2}{\sqrt{\pi}} \int_x^{\infty} \exp(-t^2) dt \quad (6)$$

while E_b/N_0 is the bit-SNR.

5. DISTANCE PROPERTIES OF TURBO CODES

There are numerous parameters that affect the performance of turbo codes. Some of them are inter-related. Hence, from now on, we shall focus our attention on the coding performance of turbo codes in conjunction with certain parameters. In this section, we first consider the effect of the distance (or weight) distribution on the coding performance. We note that, since BCH codes are employed as the component codes of the TBCH codes investigated, the distance properties of TBCH codes are similar to those of BCH codes.

5.1. Effects of Distance Spectrum

Let the transmitted codeword be an all-zero codevector, where D represents the Hamming distance of a given codeword from the all-zero codevector. Moreover, we assume that $p_{bp}(D)$ represents the union bound of the bit error probability contributed by the codewords having a distance of D from the transmitted codevector. The distribution of $p_{bp}(D)$ as a function of D is defined as the distance-spectrum, which can be expressed as:

$$p_{bp}(D) = \frac{1}{2N} W_D \cdot \mathrm{erfc}\left(\sqrt{\frac{E_b R D}{N_o}}\right), \quad (7)$$

according to Eq.(5) for $D = d_{min}, d_{min}+1, \ldots, n$. Explicitly, the union bound performance of a code is determined by the sum of all the distance-spectrum terms having Hamming distance $d_{min}, d_{min}+1, \ldots, n$. These weight-distribution terms have different degree of influence on the union bound performance. Specifically, $p_{bp}(d_{min})$ is defined as the first distance spectrum term, while $p_{bp}(d_{min}+j-1)$, $j = 1, 2, \ldots, n-k$ is defined as the jth distance spectrum term.

In turbo codes, the free distance d_{free} is defined as the minimum Hamming distance. $W_{d_{free}}$ is the total number of erroneous information databits - ie excluding the parity bits - in all codewords having a distance corresponding to the free distance from the all-zero codevector. Hence, the first distance spectrum term corresponding to the free distance is given by:

$$p_{bp}(d_{free}) = \frac{1}{2N} W_{d_{free}} \cdot \mathrm{erfc}\left(\sqrt{\frac{E_b R d_{free}}{N_o}}\right). \quad (8)$$

Fig. 2 shows the union bound BER performance of the TBCH(7,4,3) code and the BER curves corresponding to its free-distance, 2nd and 3rd distance spectrum terms as a

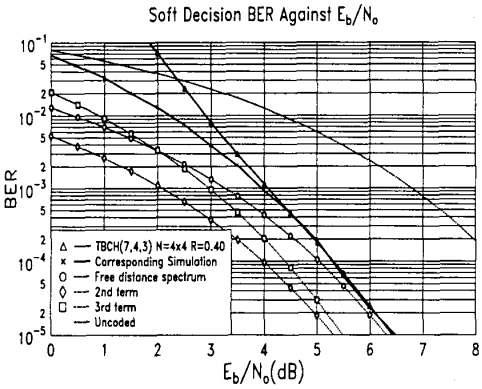

Figure 2: Union bound performance of the TBCH(7,4,3) code for an information segment size of $N = 4 \times 4$ along with its simulated performance. The associated BER of the first three distance spectrum terms is also shown, demonstrating the influence of the free-distance spectrum term on the union bound.

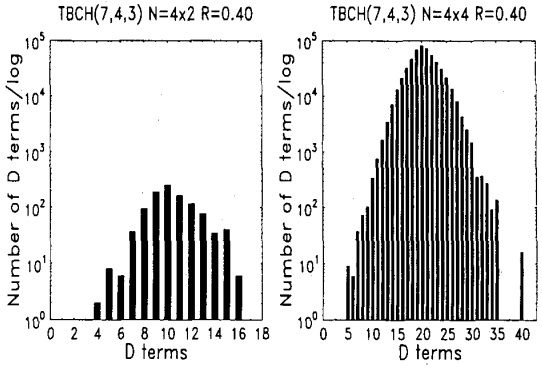

Figure 3: Weight distribution of the TBCH(7,4,3) code for $N = [4 \times 4, 4 \times 2]$, showing the effects of increasing the interleaver size, N, of the TBCH codes, which maintaining a constant coding rate, R.

function of the average SNR per bit expressed as E_b/N_0. From the results we notice that the contribution of the 2nd distance spectrum term is more considerable, than that of the 1st term, when $E_b/N_0 < 2$dB. However, the union bound is more and more dominated by the the free-distance spectrum term, when increasing the SNR per bit.

Fig. 3 shows the weight-distribution of the TBCH(7,4,3) code with interleaver size of $N = 4 \times 2$ and code rate of $R = 4/(4+3+3) = 0.40$, as well as that of the TBCH(7,4,3) code with interleaver size of $N = 4 \times 4$ and $R = 0.4$. It can be observed that the weight-distribution is significantly changed, when changing the interleaver size N. Although the code rate remained constant, i.e. $R = 0.40$ for the TBCH(7,4,3) code, d_{free} for the code with $N = 4 \times 2$ is 4, while for the code with $N = 4 \times 4$ we have $d_{free} = 5$, and their corresponding number of 'D' terms are 2 and 9, respectively.

In Fig. 4 we show the effect of the distance spectra on the bit error rate performance of the TBCH(7,4,3) code with $N = 4 \times 2$ and $N = 4 \times 4$, corresponding to the weight-distributions in Fig.3, respectively. In the figures, the influence of the first and last several distance spectrum terms was evaluated. It is clear that the BER effects of the higher-weight D-terms are less dramatic. Therefore, the distance spectrum terms corresponding to high D values have a less significant influence on the union bound BER performance. However, we observe in Fig.4 that for the TBCH(7,4,3) code having $N = 4 \times 2$, the BER-influence of the 2nd spectrum term is higher, than that of the free-distance term, when $E_b/N_0 < 5$dB. By contrast, for the TBCH(7,4,3) code having $N = 4 \times 4$, the BER-curve associated with the 3rd spectrum term is nearer to the union bound than the free-distance spectrum term related BER-curve, when $E_b/N_0 < 2$dB. These results can be explained with the aid of the corresponding weight distribution functions, which were shown in Fig.3. For the TBCH(7,4,3) code using $N = 4 \times 2$, it is observed that the second weight spectrum line is significantly higher than the first one, which consequently has a significant contribution to the bit error rate, even though the probability having five bit errors is slightly lower, than that of having four bit errors. Similarly, for the TBCH(7,4,3) code using $N = 4 \times 4$, the 3rd weight spectrum line is significantly higher than both the 1st and the 2nd weight spectrum lines, which explains the relationship amongst the various BER curves in Fig.4 for the TBCH(7,4,3) code using $N = 4 \times 4$.

Nevertheless, a weight-spectrum having a high d_{free} will result in an improved union bound BER performance. Hence, 'good' turbo codes exhibit the following properties:

1. High free distance.
2. Low 'density' of the free-distance weight spectrum term.
3. The first few weight spectrum lines exhibit low densities.

6. EFFECTS OF BLOCK INTERLEAVING

In this section the performance of various turbo codes was evaluated using different interleaving memories. For block interleaving, the information bits are written into the block interleaver on a row by row basis and then passed to the second encoder on a column by column basis. This interleaver has to be fully filled by the databits, before its contents are read out, as we discussed previously.

In Fig.5, the BER performance of the TBCH(7,4,3) code with R=0.40 and different interleaver sizes was evaluated by union-bounding and by simulations. The union bounds were computed from Eq.(5). The results show that - as expected - the BER performance of the TBCH(7,4,3) code can be improved by increasing the interleaver size. However, the incremental performance improvements are reduced, when increasing the interleaver size.

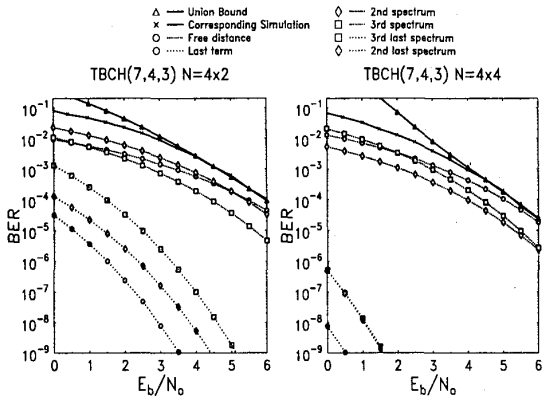

Figure 4: Union bound BER and the BER contribution of other weight-distribution terms of the TBCH(7,4,3) code for $N = [4 \times 2, 4 \times 4]$.

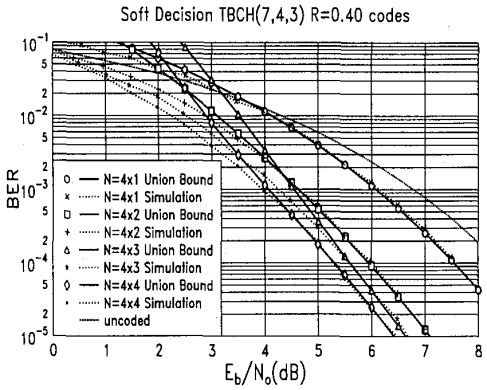

Figure 5: Comparison of union bound and simulation based BER performance for the TBCH(7,4,3) code using $N = [4 \times 1, 4 \times 2, 4 \times 3, 4 \times 4]$.

7. EFFECTS OF PUNCTURING

7.1. Puncturing Patterns

Puncturing is an often-used technique invoked, in order for a code to achieve the desired code rate. The more parity bits in the codeword of a systematic code are deleted by puncturing, the higher the code rate.

The total size of the parity section for the TBCH(7,4,3) code with interleaver size $N = 4 \times 4$ is given by Eq.(1), which is 24 bits in this case. Hence, there are $N/k = 4$ information-words in the interleaver and there are $N/k = 4$ codewords produced by each encoder, before new information databits are written into the interleaver in a new turbo encoding cycle. Each codeword has $n - k = 3$ parity bits, which are punctured according to the puncturing patterns. Hence, each puncturing pattern has $n - k = 3$ bits. If, for example, the 3 parity bits of a 7-bit codeword of the TBCH(7,4,3) code are punctured by the pattern 011_{bin}, then the codeword becomes 'ddddOpp', where 'd' represents the position of the unpunctured information databit, 'p' represents the position of the unpunctured parity bit, and '0' represents the position of the punctured parity bit. Each encoder produces $N/k = 4$ codewords at each cycle, hence there are 8 puncturing patterns associated with the 8 original BCH codewords for the two encoder outputs. Let us represent the puncturing patterns by $[P_1P_1P_1,\ P_1P_1P_1,\ P_1P_1P_1,\ P_1P_1P_1,\ P_2P_2P_2,\ P_2P_2P_2,\ P_2P_2P_2,\ P_2P_2P_2]_{bin}$, which represents the $8 \times 3 = 24$ parity bits of a turbo-coded word, where P_1 represents the parity of the first encoder and P_2 that of the second encoder. These binary puncturing patterns are then converted into hexadecimal form for reasons of compactness.

7.2. Performance of Puncturing

As we discussed at the beginning of this section, puncturing a codeword results in a trade-off between transmission efficiency and coding performance. This phenomenon is explicitly portrayed in Fig. 6, where the BER performance of the TBCH(7,4,3) code is enhanced, as the code rate is decreased by transmitting more parity bits, i.e., by increasing the value of p_w in Eq.(4). Note that the puncturing patterns in the figure are expressed in hexadecimal form.

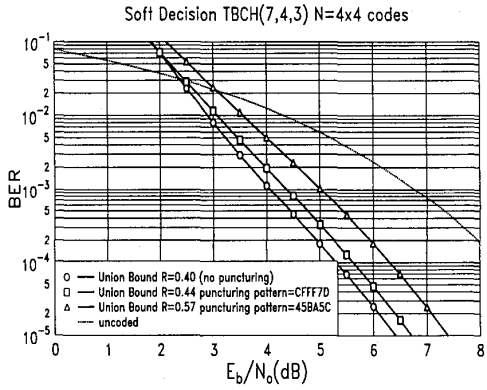

Figure 6: Union bound BER performance of the TBCH(7,4,3) code using an $N = 4 \times 4$ interleaver for R=[0.41,0.44,0.57], showing the effect of puncturing by increasing the coding rate, R.

We also note that the BER performance of a turbo code having a fixed code rate depends on the specific puncturing pattern employed. Fig.7 demonstrates this effect, where the results were computed according to Eq.(5), indicating that the performance of the codes may differ significantly by applying different puncturing patterns. Hence, for each application the optimum puncturing patterns have to be found.

For the TBCH(7,4,3) code using an interleaver size of $N = 4 \times 4$ and $p_w = 12$, when half of the parity bits are deleted, the optimum puncturing patterns have been ob-

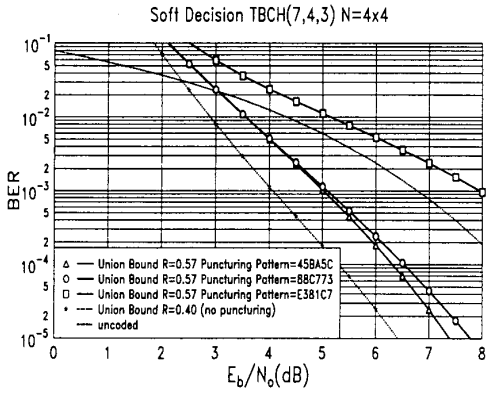

Figure 7: Union bound BER performance of the TBCH(7,4,3) code using an $N = 4 \times 4$ interleaver and a range of puncturing patterns with $R = 4/7$, showing the effect of puncturing at a constant coding rate, R.

tained, which are in Table 1. It can be expressed as 45BA5C in hexadecimal form, or 010001011011101001011100=45BA5C in the binary form, as shown in Fig.7. This pattern results in $d_{min} = 3$, which is the highest possible distance that could be found for all puncturing patterns associated with $p_w = 12$. The corresponding weight density is $W(d_{min}) = 20$, which is the lowest possible value for the punctured code with $d_{min} = 3$ that can be achieved.

Encoder	*databits*	*parity bits*
1*st*	dddd	010
	dddd	001
	dddd	011
	dddd	011
2*nd*	xxxx	101
	xxxx	001
	xxxx	011
	xxxx	100

Table 1: The optimum puncturing patterns of the TBCH(7,4,3) code using $N = 4 \times 4$, where 'd' and 'x' represent the positions of the original information databit and the interleaved information databit, respectively, while '1' and '0' represent the positions of the unpunctured and punctured parity bits, respectively. The puncturing pattern can be expressed as 45BA5C in hexadecimal form.

8. SUMMARY AND CONCLUSION

Our discussions have been focused on analysing the performance and weight distribution of short block based turbo codes. The effect of turbo interleaving and puncturing were studied. We found that there is a certain grade of freedom in shaping the weight distribution and hence the BER curve. However, further study is required, in order to improve the TBCH code design flexibility by facilitating a more 'bespoke' BER curve design for specific applications. A range of algorithms that can be used for decoding the TBCH codes studied in this contribution were characterised in [10], while as an application example, an adaptive-rate turbo block coded transceiver was proposed and investigated in [11].

9. REFERENCES

[1] C. Berrou, A. Glavieux and P. Thitimajshima, "Near Shannon Limit Error-Correcting Coding and Decoding : Turbo Codes", in *IEEE Proceedings of ICC'93*, pp.1064-1070, 1993.

[2] S. Benedetto and G. Montorsi, "Unveiling Turbo Codes: Some Results on Parallel Concatenated Coding Schemes", *IEEE Transactions on Information Theory*, Vol.42, No.2, pp.409-428, Mar. 1996.

[3] S. Benedetto and G. Montorsi, "Generalized Concatenated Codes with Interleavers", in *International Symposium on Turbo Codes and related topics*, pp.32-39, France: Brest, Sept. 1997.

[4] C. Schlegel, *Trellis Coding*, pp.233-263, New York, 1997.

[5] R. M. Pyndiah, "Near-Optimum Decoding of Product Codes: Block Turbo Codes," *IEEE Transactions on Communications*, pp. 1003-1010, August 1998.

[6] J. Hagenauer, E. Offer and L. Papke, "Iterative Decoding of Binary Block and Convolutional Codes," *IEEE Trans. on Infor. Theory*, Vol.42, No.2, pp.429-445, Mar. 1996.

[7] J. Yuan, B. Vucetic and W. Feng, "Combined Turbo codes and interleaver design," *IEEE Trans. on Commun.*, Vol.47, No.4, pp.484-487, Apr. 1999.

[8] R. Steele and L. Hanzo, *Mobile Radio Communications*, 2nd Ed. IEEE Press, New York, 1999.

[9] J. G. Proakis, *Digital Communications*, (3rd Ed.) New York: McGraw-Hill, 1995.

[10] T.H. Liew, L-L. Yang, L. Hanzo, "Iterative decoding of redundant residue number system codes", in this Proceedings

[11] T. Keller, T.H. Liew, L. Hanzo, "Adaptive Rate RRNS Coded OFDM Transmission for Mobile Communication Channels", in this Proceedings